Variability of the F1 Ionospheric Layer During Periods of Quiet and Shock Geomagnetic Activity at the Korhogo station.

Abstract

In this work, the diurnal variability of the critical frequency foF1 and the virtual height h'F1 is studied above the Korhogo equatorial station (Côte d'Ivoire) during periods of quiet and shock geomagnetic activity. The study days were identified using pixel diagrams and the classification of Legrand and Simon (1989). The analyses were conducted according to the seasons and solar phases, based on mean diurnal profiles. The results show that during quiet periods, the F1 layer exhibits regular diurnal profiles, predominantly dome-shaped, with a strong seasonal and solar dependence of foF1, confirming the dominance of photochemical processes. Conversely, during periods of shock activity, significant perturbations are observed, characterized by ionization troughs, compressions, and vertical instabilities of h'F1, as well as a reduction in the lifespan of the F1 layer, particularly in summer and at solar maximum. These signatures reveal the combined influence of penetrating electric fields, perturbed thermospheric winds, and enhanced recombination processes on the dynamics of the equatorial F1 layer.

Keywords: Equatorial ionosphere, F1 layer variability, Geomagnetic shock activity, foF1 and h'F1

I. Introduction

The F1 ionospheric layer, located between 150 and 220 km altitude, originates primarily from photoionization induced by solar ultraviolet and extreme ultraviolet radiation. Unlike the F2 layer, which is strongly influenced by dynamic processes such as thermospheric winds and electric fields, the F1 layer is essentially controlled by photochemical processes. This photochemical dominance results in relatively low variability and a strong dependence on solar irradiance, as demonstrated by Rishbeth and Garriott (1969), Kelly (2009), and Yiğit et al. (2018).

Furthermore, the F1 layer plays a fundamental role as a transition zone between the ionospheric region dominated by photochemistry and the upper region where plasma transport processes become predominant. It is therefore an essential region for understanding vertical plasma exchange between the F1 and F2 layers, particularly in regions affected by the equatorial ionospheric anomaly (Ouattara and Amory-Mazaudier, 2012).

From an application perspective, the F1 layer contributes to the overall structuring of the daytime electronic profile and influences the propagation conditions of high-frequency (HF) radio waves. Although it is not the primary reflective layer, its presence and variations can modify absorption mechanisms and indirectly affect the quality of radio communications in equatorial environments.

Furthermore, it is important to emphasize that during periods of intense geomagnetic activity, particularly during shock activity, the hypothesis of the F1 layer's near-total insensitivity to magnetic perturbations (Mikhailov and Schlegel, 2002) warrants re-examination. Indeed, shock activity is accompanied by abrupt variations in the dynamic pressure of the solar wind, inducing penetrating electric fields and thermospheric perturbations that can temporarily alter the photochemical equilibrium of the F1 region. The response of this layer during these transient phases remains poorly documented, especially in the African context. This work aims to study the variability of the F1 layer above Korhogoionosonde station (Lat. 9.3°N; Long. 354.6°E; dip. 0.6°S) during quiet and shock geomagnetic activity. The study relies on the ionospheric parameters foF1 and h'F1 to further characterize the response of this layer to geomagnetic perturbations and contribute to a better understanding of the equatorial ionospheric climate.

II. Data and Methods

II.1. Data

In this study, aa index data were used to construct pixel diagrams, which allowed for the extraction of days corresponding to quiet and shock geomagnetic activity. The aa index data were provided by ISGI (International Service of Geomagnetic Indices) via the link https://isgi.unistra.fr/data_download.php.

The foF1 and h'F1 parameters were used to evaluate the ionization intensity, the vertical dynamics of the F1 layer, and its response to geomagnetic storms. Data for these parameters were recorded from 1992 to 2002 at the Korhogo ionosonde station (Lat. 9.3°N; Long. 354.6°E; dip. 0.6°S), Republic of Côte d'Ivoire (RCI). This station is located in the trough of the Equatorial Ionization Anomaly (EIA). The data for these parameters are available on the GIRGEA website at https://www.girgea.org/recherches/logiciels/

The Rz index was used to identify solar phases. Data for this index were provided by OMNIWEB via the following link: https://omniweb.gsfc.nasa.gov/form/dx1.html

II.2. Methods

Days of geomagnetic activity: The identification of days of geomagnetic activity was carried out using pixel diagrams. This graphical method, introduced by Legrand and Simon (1989) and widely used in the West African sector (Zerbo et al., 2012; Ouattara and Amory-Mazaudier, 2009; Kaboré et al., 2021; Diabaté et al., 2025), allows visualization of days of geomagnetic activity based on daily values of the aa index, color-coded. The classification criteria defined by Legrand and Simon (1989) and adopted by Zerbo et al. (2012) were used. According to these criteria, days of quiet activity correspond to days with an Aa index ≤ 20 nT; days of shock activity correspond to days of sudden storm commencement (SSC**)** with the Aa index ≥ 40 nT. Figure 1 is a pixel diagram of the year 1993. In this figure, three days of shock activity (January 19-20, 1993) and four days of quiet activity (February 3-6, 1993) are identified.

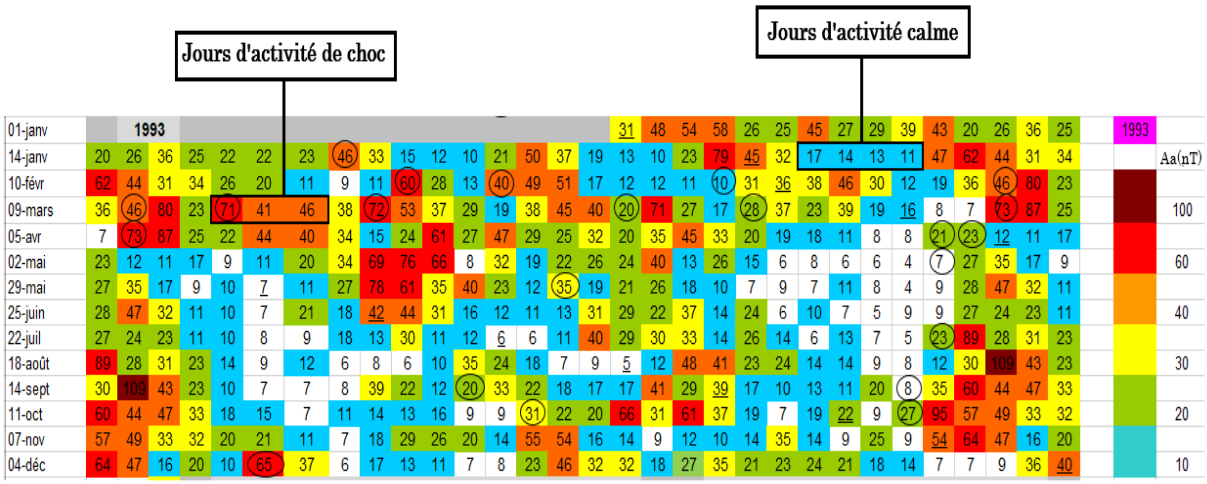

Figure 1: Pixel diagram for the year 1993. Three days of shock activity and four days of calm activity are identified.

Identification of solar phases: The criteria defined by Sawadogo et al. (2024) were used to identify the different solar phases. Table 1 presents the distribution of the study years by solar phase according to this criterion.

Table 1: Solar phases and corresponding years

Cycle Phase	Years	**Criteria on Rz**
Descending	1992-1995	$100 \geq Rz \geq 20$
Minimum	1996	$Rz < 20$
Ascending	1997-1998	$20 \leq Rz \leq 100$
Maximum	1999-2002	$Rz > 100$

Season identification: For the seasonal study, the months of the year were classified by season. Thus, we have winter (December, January, February), spring (March, April, May), summer (June, July, August), autumn (September, October, November).

Diurnal profiles: The diurnal profiles were obtained from the daily arithmetic means of foF1 and h'F1 for each solar phase and for each season. These means were calculated using equations (1) and (2).

$$foF1 = \frac{\sum_{i=0}^{i=n+1} foF1_i}{n} \quad (1)$$

$$h'F1 = \frac{\sum_{i=0}^{i=n+1} h'F1_i}{n} \quad (2)$$

foF_{1i} and $h'F_{1i}$ are respectively the values of foF1 and h'F1 at time i, n is the number of terms (n = 25).

Analysis and interpretation method: Diurnal profiles were analyzed to identify the main perturbation signatures. Comparative analyses were performed according to the seasons and phases of the solar cycle. The diurnal profiles of foF1 were analyzed in light of the profiles defined by Faynot and Vila (1979) in the equatorial region. The observed variations were interpreted in terms of known ionospheric perturbation mechanisms, such as penetration electric fields, perturbed thermospheric winds, E×B drifts, and induced ionospheric currents.

III. Results and Discussion

III.1. Variations in foF1 and h'F1 during periods of low activity

III.1.1. Seasonal Variations

Figure 2 shows the seasonal diurnal variations of foF1 and h'F1 during periods of low activity. Panels a, b, c, and d represent the profiles for winter, spring, summer, and autumn, respectively. The blue and red curves represent the daily profiles of foF1 and h'F1, respectively.

On all panels, the foF1 profiles show almost the same trend. Indeed, they are all dome-shaped. However, in summer and spring, a slight dip in ionization is observed around noon (11:00–14:00 UT). Also note that the heights of the domes vary from one season to another, thus characterizing a seasonal dependence of ionization during periods of low activity. Furthermore, this ionization is more pronounced in summer and spring, with ionization maxima (3.2 MHz and 3.3 MHz) reached around 12:00 UT. Ionization is less significant in winter, with a maximum of 1.9 MHz reached at 12:00 UT,consistent with observations made by Somoye (2016). These seasonal variations reflect (1) the variation in solar EUV flux and solar zenith angle (Rishbeth and Garriott, 1969), (2) the geographical position of the Korhogo station (near the magnetic equator) under the influence of the EXB drift (Balan et al., 1995; Oyekola, 2008), and (3) marked ionization in summer due to the solar tilt. These observations show that during periods of quiet activity, the critical frequency foF1 is weakly influenced by thermospheric dynamics, while it is mainly controlled by solar radiation.

The h'F1 profiles are characterized by a trough around 6:00 UT, two peaks at 7:00 and 8:00 UT respectively, a plateau at midday (10:00 –12:00 UT), followed by a decrease during the night (20:00 – 00:00 UT) and the morning (00:00–6:00 UT), indicating the gradual reappearance of recombination dominance. It should be noted that the intensity of the peaks and troughs is seasonal. According to some authors, the trough around 6:00 UT is the signature of a nocturnal-diurnal transition phase (Buresova 2002; Mikhailov 2008; Lastovicka 2006), and the 7:00 UT peak corresponds to the initial rapid rise of the thermosphere just after dawn (Hargreaves, 1992; Kelly, 2009). Indeed, during the night, recombination lowers the density and structure of the ionosphere, and then at sunrise, the rise in ionization takes some time to restore the vertical distribution. This delay can cause a trough in h'F1 just before the onset of ionization.

During periods of quiet geomagnetic activity, the diurnal and seasonal variations in foF1 and h'F1 at Korhogo confirm that the F1 layer is primarily governed by solar photochemical processes, modulated by the thermospheric structure and equatorial electrodynamic effects. These results thus fit within the equatorial ionospheric climatology described by Rishbeth& Garriott (1969) and Rishbeth& Mendillo (2001).

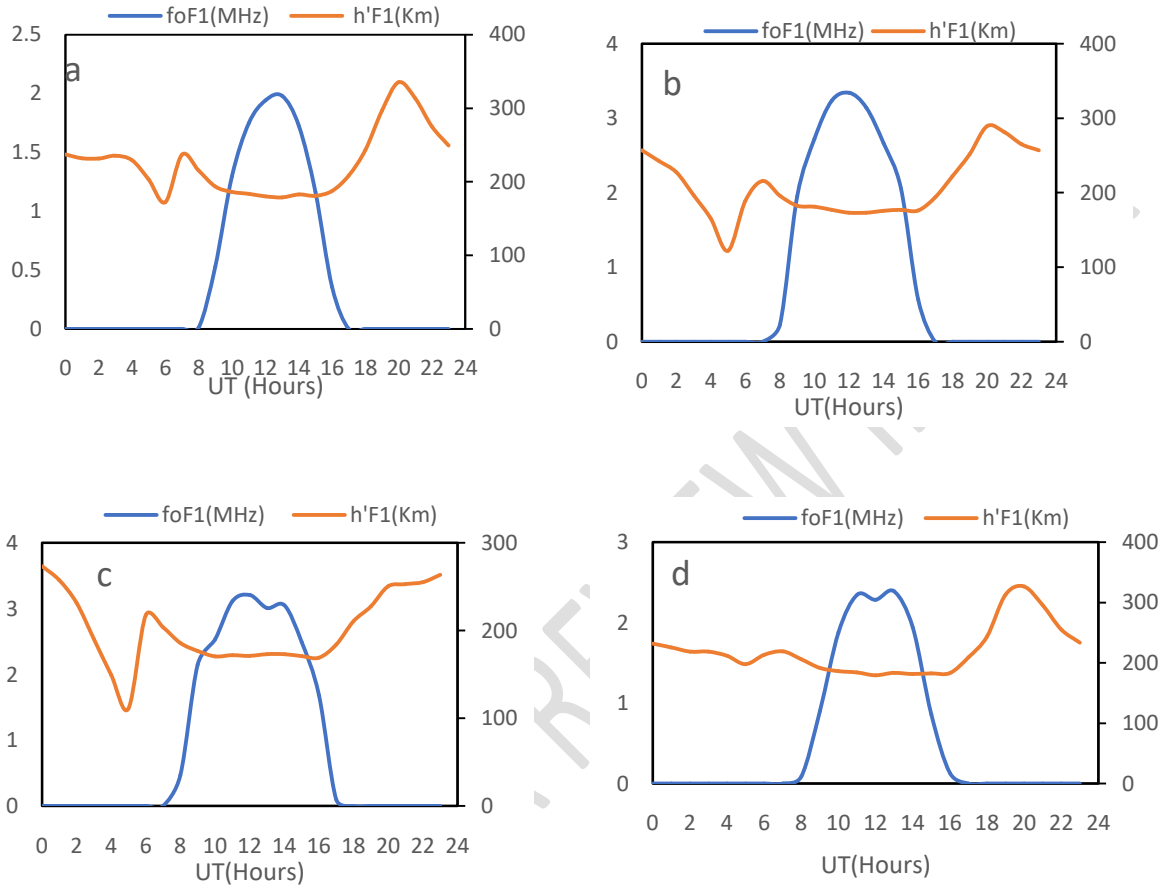

Figure 2: Seasonal diurnal profiles of foF1 and h'F1 during periods of low activity; a: winter profile, b: spring profile, c: summer profile, d: autumn profile

III.1.2. Variations by Solar Phase

Figure 3 shows the diurnal variations by solar phase of foF1 and h'F1 during periods of low activity. Panels a, b, c, and d represent the profiles at solar minimum, ascending, maximum, and descending phases, respectively. The blue and red curves represent the daily profiles of foF1 and h'F1, respectively.

At solar minimum (Panel a), the diurnal profiles of foF1 are characterized by two peaks of 4.0 MHz at 12:00 and 4.0 MHz at 14:00 (UT), followed by a small ionization trough (< 1 MHz) around 13:00. Its lifetime is 9 hours (7:00–17:00 UT). The h'F1 profile shows a trough (80 km) at 5:00 (UT) and two peaks (217 and 247 km) at 7:00 and 20:00 (UT), respectively. The double crest of foF1 suggests a complex modulation of ionospheric production, probably

linked to local dynamic effects (neutral wind, electric field) (Laštovička, 2006; Ouattara et al., 2012).

During the rising phase (Panel b), the foF1 profile appears around 08:00 (UT) and then increases rapidly, reaching a maximum of 3 MHz between 10:00 and 12:00 (UT). It gradually decreases in the afternoon and disappears around 17:00 (UT). This behavior is typical of an F1 layer controlled primarily by solar photoionization. The h'F1 profile oscillates around 180–250 km, with a slight decrease in the middle of the day and a relative increase in the morning and late afternoon. This low variability of h'F1 indicates, on the one hand, a relatively stable altitude of the F1 layer and, on the other hand, variability dominated by chemical equilibrium rather than by vertical transport of the ionospheric plasma (Mostafa et al., 2017).

At solar maximum (Panel c), the foF1 profile is characterized by a very weak maximum (0.5 MHz) at noon (12:00 UT) and an existence duration of 8 hours (9:00–17:00). The h'F1 profile shows that the F1 layer is higher (250–330 km) and exhibits stable variability compared to other solar phases. Ionization of the F1 layer is less pronounced, despite the solar maximum. This result is consistent with Kim et al. (2020), Yiğit et al. (2018), and Rishbeth and Setty (1961), who suggest this observation is due to the dominance of the F2 layer, which absorbs or masks the characteristics of F1. The stability of h'F1 suggests a more homogeneous structuring of the ionospheric region.

During the descending phase (Panel d), the foF1 profile is characterized by a less pronounced trough around noon (12:00 UT), maxima around the trough (3.5 and 4 MHz), and a duration of approximately 10 hours (7:00–17:00 UT). The h'F1 profile exhibits the same characteristics as the preceding phases but with average extreme values (200–300 km). The descending phase maintains significant ionospheric activity, with a well-defined F1 structure. The central trough could be related to recombination effects or a transition toward F2 layer dominance (Mikhailov 2008; Balan and Bailey, 1995).

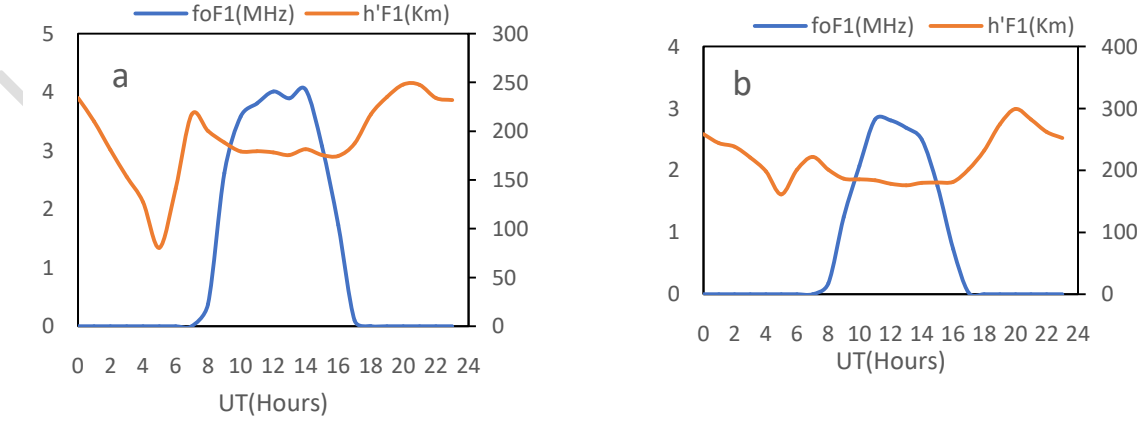

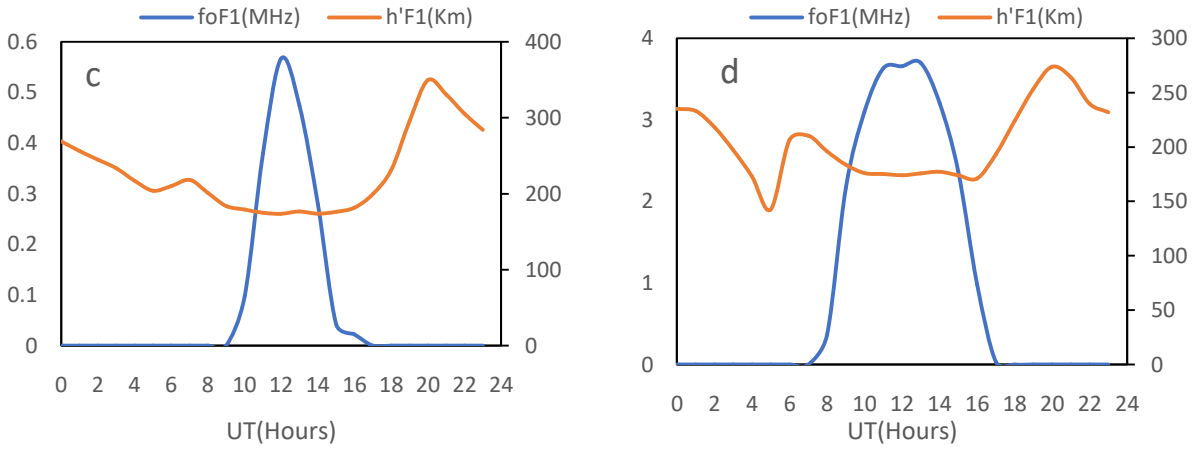

Figure 3: Diurnal profiles by solar phase of foF1 and h'F1 during periods of quiet activity; a: solar minimum profile, b: ascending phase profile, c: solar maximum profile, d: descending phase profile.

III.2. Variations in foF1 and h'F1 during periods of shock activity

III.2.1. Seasonal variations

In winter (Panel a), the foF1 profile shows a high peak (~2–2.5 MHz) centered around noon. The F1 layer exists between 9:00–16:00 (UT). The h'F1 profile drops around the peak (compression) but exhibits two notable peaks (213 and 266 km) at 7:00 and 20:00 (UT) respectively, followed by a trough at 6:00 (UT). These observations indicate that geomagnetic activity intensifies diurnal densification, inducing uplift and compression phenomena, which may be associated with generated ionospheric currents (Buresova et al. 2002; Paul et al. 2025), Barad et al. (2025)

In spring (Panel b), the foF1 profile shows two notable peaks (2.3 and 2.6 MHz) at 11:00 and 13:00(UT), respectively, followed by a fairly significant ionization trough (<1 MHz) at 12:00(UT). The F1 layer persists between 8:00 and 4:00 (UT). The h'F1 profile shows more pronounced fluctuations and a slight dip around noon (130 km) compared to the winter profile. The ionization trough observed at noon UT on the foF1 profile could result from an EXB drift, which lifts the ionospheric plasma to higher altitudes, temporarily reducing the density in the F1 layer (Fejer et al., 2011; Zerbo et al., 2012).

In summer (Panel c), the foF1 profile is characterized by very weak peaks (max < 0.9 MHz) and a notable ionization trough at 14:00 (UT), consistent with Lobzin and Pavlov (2002). A narrow and short profile is also observed (late appearance ≈ 10:00–11:00(UT), disappearance ≈ 15:00–16:00 → 5:00: –6:00 (UT)). The h'F1 profile is high (260 km) and relatively variable. These observations indicate that geomagnetic activity strongly disrupts the formation of the F1 layer, with a delay in its appearance and vertical instability, probably linked to the effects of shock activity (Mikhailov and Schlegel, 2002; Paul et al., 2025).

In autumn (Panel d), the foF1 profile is characterized by a notable peak (≈1.8–2 MHz) around noon with a rapid decay in the afternoon and a duration similar to spring (≈08:00–17:00 UT).

The h'F1 profile shows the same trends as in winter but with low variability. These observations indicate a relatively low variability in foF1 and a reduction in the duration of the F1 layer, probably linked to faster recombination. The seasonal profiles of foF1 and h'F1 at Korhogo during periods of shock activity thus reveal a strongly perturbed ionospheric dynamic. The observed signatures — compression, ionization troughs, vertical instability — confirm the effects of shock activity on the F1 layer, in contrast to the more regular profiles in calm periods.

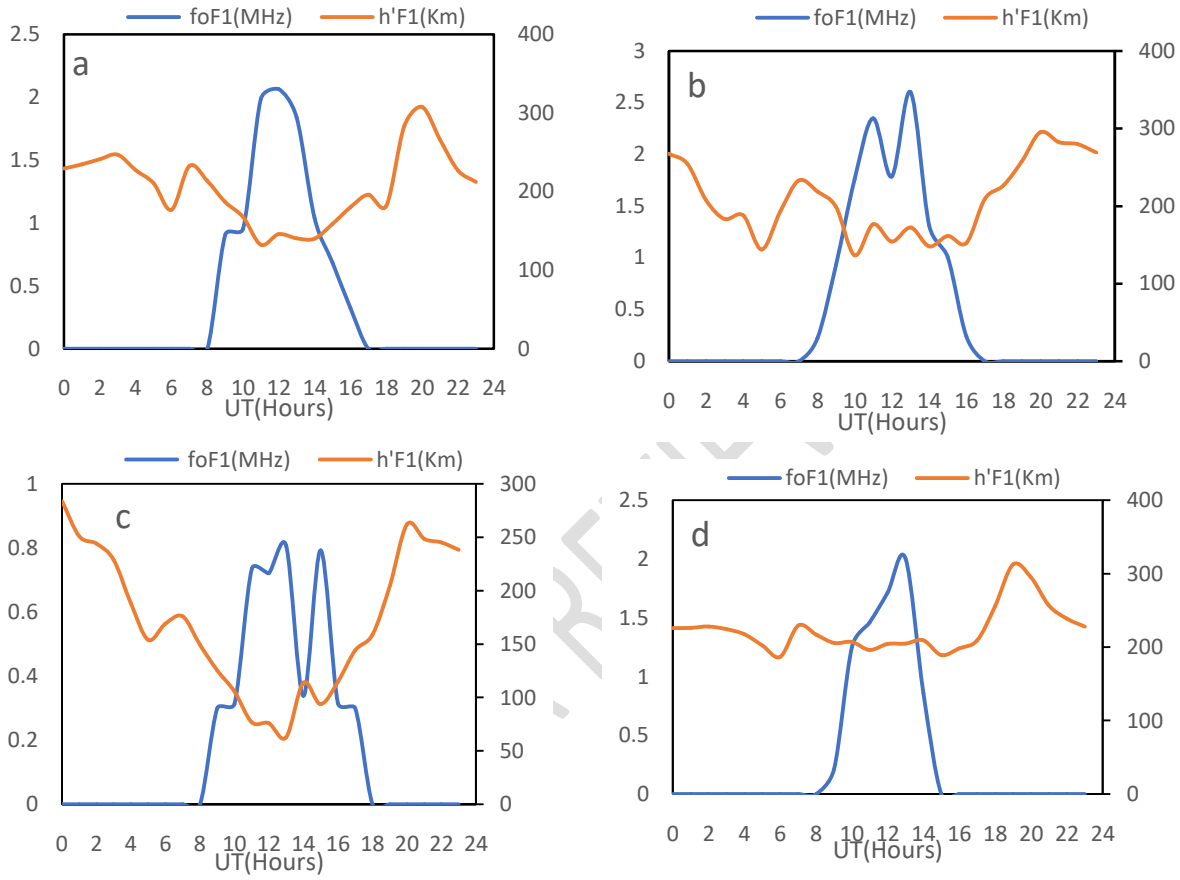

Figure 4: Seasonal diurnal profiles of foF1 and h'F1 during periods of shock activity; a: winter profile, b: spring profile, c: summer profile, d: autumn profile

III.2.2. Variations by Solar Phase

Figure 5 shows the diurnal variations by solar phase of foF1 and h'F1 during periods of low activity. Panels b, c, and d represent the profiles at the ascending, maximum, and descending solar phases, respectively. The blue and red curves represent the daily profiles of foF1 and h'F1, respectively. No results are available for solar minimum because we did not observe any days of shock activity during this solar phase. This could be due to the fact that during the study period (1992–2002), there were no geoeffective CMEs during this solar phase (Legrand and Simon 1989; Richardson and Cane 2010; Tsurutani et al., 2006).

During the ascending phase (panel b), the foF1 profile is characterized by a peak (3.28 MHz) around 13:00 (UT), the presence of oscillations (9:00 UT), and a significant duration of approximately 10 hours (7:00-17:00 UT). The h'F1 profile is characterized by strong compression between 8:00-12:00(UT), a descent to 200 km, and a rise after 14:00 (UT), a signature of post-perturbation relaxation. These observations indicate an increase in ionization processes linked to the rise in solar activity, the existence of rapid perturbations, and neutral equatorial winds disturbed by shock activity.

At solar maximum (Panel c), the foF1 profile is more regular, significantly less pronounced than during the ascending phase (0.4 MHz), and has a very short duration (8 hours). The h'F1 profile is characterized by a marked depression around 12:00-14:00 UT (180-190 km), which is more stable and lower, indicating a highly compressed ionosphere.

During the descending phase (Panel d), the foF1 profile exhibits a double peak (2.4 MHz) at 11:00 and 13:00 (UT) and an ionization trough at 12:00 (UT). This profile lasts 10 hours (8:00 -18:00 UT). The h'F1 profile is marked by moderate variability and a slight compression (150-280 km), indicating progressive relaxation.

Analysis of foF1 and h'F1 profiles at the Korhogo station during periods of shock activity reveals (1) greater h'F1 compression, characteristic of increased neutral density (Fuller-Rowell and Evans, 1994), and (2) more pronounced diurnal oscillations, indicating the influence of atmospheric perturbations generated by shock activity (Hunsucker, 1982). We also note (3) less pronounced foF1 values at solar maximum, likely linked to combined effects of shock activity at solar maximum on the thermosphere's composition, which favor recombination at the expense of ionization (Klimenko et al., 2018).

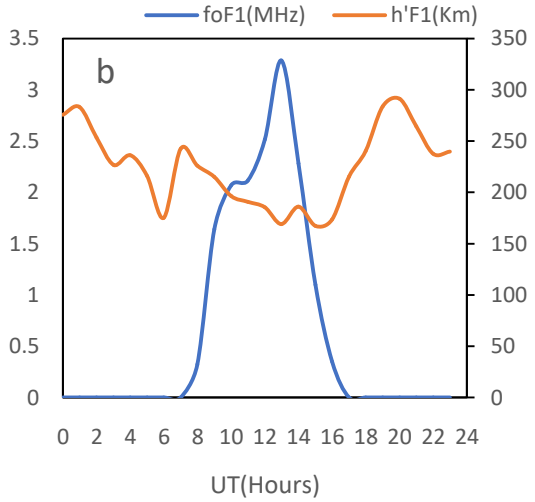

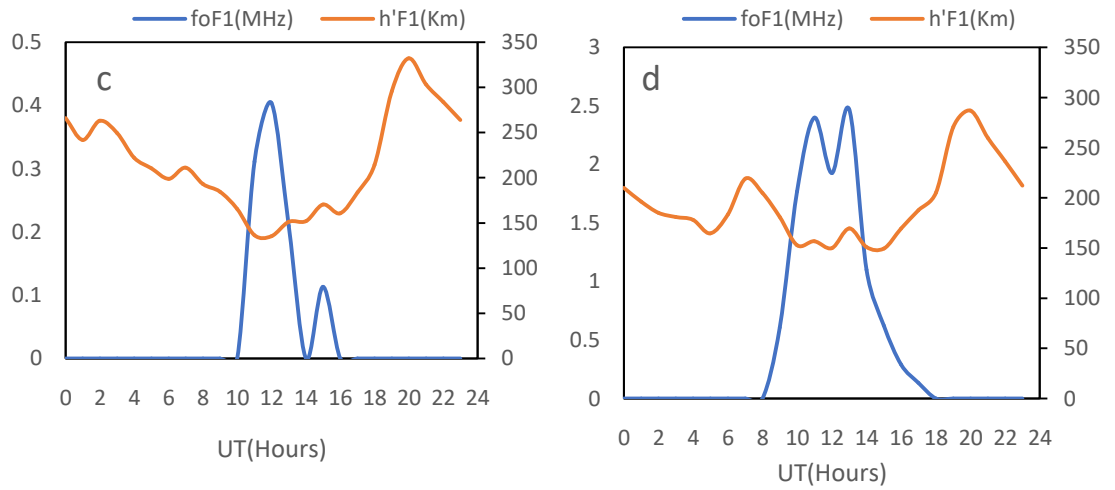

Figure 5: Diurnal profiles of foF1 and h'F1 during the different solar phases during periods of shock activity; a: Profile during the ascending phase, b: Profile at solar maximum, c: Profile during the descending phase.

VI. Conclusion

This study characterized the diurnal, seasonal, and solar variability of the F1 ionospheric layer above Korhogo by comparing its responses to conditions of quiet and shock geomagnetic activity. The results confirm that during quiet periods, the F1 layer is primarily governed by solar photochemical processes, with regular foF1 profiles and a relatively stable vertical h'F1 structure, modulated by the seasons and phases of the solar cycle. Conversely, during periods of shock activity, the F1 layer exhibits increased sensitivity to rapid geomagnetic perturbations. The observed signatures—ionization troughs, h'F1 compressions, vertical instabilities, and a reduction in the layer's lifetime—indicate a temporary disruption of photochemical equilibrium under the influence of penetrating electric fields, perturbed thermospheric winds, and variations in neutral composition. These effects are particularly pronounced in summer and at solar maximum, when the dominance of the F2 layer tends to mask or weaken the characteristics of the F1 layer. These results highlight that, contrary to the hypothesis of the F1 layer's near-insensitivity to geomagnetic perturbations, shock activity can significantly alter its dynamics, even at low latitudes. This work thus contributes to equatorial ionospheric climatology in West Africa and underscores the importance of integrating the F1 layer into studies of the impact of rapid geomagnetic perturbations.

Acknowledgments

The authorsacknowledge OMNIWEB for providing the Rz and aa index data, and GIRGEA for providing the foF1 and h'F1 data

References

Balan N. and Bailey G.J. (1995). Equatorial plasma fountain and its effects: Possibility of an additional layer. Journal of Geophysical Research: Space Physics/ Vol. 100(A11): 21421-21432. https://doi.org/10.1029/95JA01555

Barad K.R., Sripathi S., Singh R., Gayathri B., Abadi P. (2025). Observations and Modeling Investigations of Ionospheric Response to 23–24 April 2023, G4-Class Geomagnetic Storm Over Indian Sector. Vol. 23(6). https://doi.org/10.1029/2024SW004253

Buresova J., Lastovicka J., Altadill D. and Miro G. (2002). Daytime electron density at the F1-region in Europe during geomagnetic storms. Annales Geophysicae (2002) 20: 1007–1021.

Diabaté A., Sawadogo W.E., Guibula K. And Ouattara F. (2025). Variation of the critical frequency of the ionospheric F2 layer during moderate geomagnetic conditions: A study using data from the Ouagadougou ionosonde station across solar cycles 21 and 22. Current Journal of Applied Science and Technology, 44(1): 76-86. https://doi.org/10.9734/cjast/2025/v44i14477

Faynot, J.M. and Vila, P. (1979) F-Region at the Magnetic Equator. Annales Geophysicae, 35, 1-9.

Fejer, B.G. (2011). Low Latitude Ionospheric Electrodynamics. Space Sci Rev 158, 145–166. https://doi.org/10.1007/s11214-010-9690-7

Fuller-Rowell, T.J., Evans, D.S. (1994). Response of the thermosphere and ionosphere to geomagnetic storms. Journal of Geophysical Research: Space Physics/vol. 99(A3):3893-3914. https://doi.org/10.1029/93JA02015

Hargreaves, J. K. (1992). The Solar-Terrestrial Environment: An Introduction to Geospace – the Science of the Terrestrial Upper Atmosphere, Ionosphere, and Magnetosphere. Cambridge University Press, Cambridge, 436 pp.

Hunsucker, R.D. (1982). Atmospheric gravity waves generated in the high-latitude ionosphere: A review. Reviews of Geophysics. Vol. 20(2): pp. 293-315. https://doi.org/10.1029/RG020i002p00293

Kaboré S., Guibula K., Zerbo J.L. and Ouattara F. (2021). Solar activities and geomagnetism: Long-term statistical study of magnetics clouds activity day's occurrence as a function of the phases of solar cycles 11 to 24. International Journal of Physical Sciences. Vol. 16(4), pp: 180-187. https://doi.org/10.5897/IJPS2021.4973

Kelly, M. C. (2009). The Earth's Ionosphere: Plasma Physics and Electrodynamics (2nd ed.). Academic Press (Elsevier), Amsterdam, 556 pp.

Kim E, Jee G., Ji E-Y, Kim Y.H., Lee C., Kwak Y-S. And Shim J-S. (2020). Climatology of polar ionospheric density profile in comparison with mid-latitude ionosphere from long-term observations of incoherent scatter radars: A review. Journal of Atmosphere and Solar-Terrestrial Physics. Vol. 211, 105449. https://doi.org/10.1016/j.jastp.2020.105449

Klimenko, M.V., Kilmenko V.V., Despirak I.V., Zakharenkova I.E., Kozelov B.V., Cherniakov S.M., Andreeva E.S., Tereshchenko E.D., Vesnin A.M., Korenkova N.A., Gomonov A.D., Vasiliev E.B., Ratovsky K.G. (2018). Disturbances of the thermosphere-ionosphere-plasmasphere system and auroral electrojet at 30°E longitude during the St. Patrick's Day geomagnetic storm on 17–23 March 2015 Journal of Atmospheric and Solar-Terrestrial Physics. Vol. 180, pp. 78-92. https://doi.org/10.1016/j.jastp.2017.12.017

Laštovička, J. (2006). Forcing of the ionosphere by waves from below. Journal of Atmospheric and Solar-Terrestrial Physics 68(3): 479-497, https://doi.org/10.1016/j.jastp.2005.01.018

Legrand J.P. and Simon P.A. (1989). Solar Cycle and Geomagnetic Activity: A Review for Geophysicists. Part I. The Contributions to Geomagnetic Activity of Shock Waves and of the Solar Wind, Annales Geophysicae, vol.7, issue.6, pp.565-578.

Lobzin, V.V., Pavlov, A.V. (2002). Solar zenith angle dependencies of F1-layer, NmF2 negative disturbance, and G-condition occurrence probabilities. ANGEO, 20, 1821-1836. https://doi.org/10.5194/angeo-20-1821-2002

Mikhailov, A.V., Schlegel, K. (2002). Geomagnetic storm effects at F1-layer heights from incoherent scatter observations. Annales Geophysicae (2003) 21: 583–596. https://doi.org/10.5194/ANGEO-21-583-2003

Mikhailov, A. V. (2008). Ionospheric F1 layer long-term trends and the geomagnetic control concept. Annales Geophysicae, 26, 3793–3803. https://doi.org/10.5194/angeo-26-3793-2008

Mostafa, H., Haralambous H. And Oikonomou C. (2017). Evaluation of RI predicted characteristics of ionospheric F1 layer by ionosonde observations in Nicosia, Cyprus. Advanced in Space Research, Vol. 59(6): 1548-1558

Ouattara, F., Amory-Mazaudier, C. (2009). Solar–geomagnetic activity and Aa indices toward a standard classification. Journal of Atmospheric and Solar-Terrestrial Physics 71, 1736-1748. https://doi.org/10.1016/j.jastp.2008.05.001

Ouattara, F., Amory-Mazaudier, C. (2012). Statistical study of the equatorial F2 layer critical frequency at Ouagadougou during solar cycles 20, 21 and 22, using Legrand and Simon's classification of geomagnetic activity. J. Space Weather Space Clim. 2 (2012) A19. http://dx.doi.org/10.1051/swsc/2012019

Ouattara F. Gnabahou D.A. and Amory-Mazaudier C. (2012). Seasonal, Diurnal, and Solar-Cycle Variations of Electron Density at Two West Africa Equatorial Ionization Anomaly

Stations. International Journal of Geophysics, Volume 2012, Article ID 640463, 9 pages, https://doi.org/10.1155/2012/640463

Paul K.S., Haralambous H., Moses M. and Tripathi S.C. (2025). Effects of the October 2024 Storm over the Global Ionosphere, Remote Sens. 7(13), 2329. https://doi.org/10.3390/rs17132329

Richardson, I.G., Cane, H.V. (2010). Near-Earth Interplanetary Coronal Mass Ejections During Solar Cycle 23 (1996 – 2009): Catalog and Summary of Properties. Sol Phys 264, 189–237. https://doi.org/10.1007/s11207-010-9568-6

Rishbeth H. And Mendillo, M. (2001). Patterns of F2-layer variability. Journal of Atmospheric and Solar-Terrestrial Physics 63(15): 1661-1680. https://doi.org/10.1016/S1364-6826(01)00036-0

Rishbeth H. And Setty C.S.G.K. (1961). The F-layer at sunrise. Journal of Atmospheric and Terrestrial Physics. Vol. 20(4) pp. 263-276. https://doi.org/10.1016/0021-9169(61)90205-7

Rishbeth, H., & Garriott, O. K. (1969). Introduction to Ionospheric Physics. International Geophysics Series (Vol. 14). Academic Press, New York, 331 pp

Sawadogo, P., et al. (2024). Solar activity: Towards a standard classification of solar phases from cycle 1 to cycle 24. Advances in Space Research 73(8). https://doi.org/10.1016/j.asr.2023.11.011

Somoye E.O., Onori E.O., Ogahi C.O., Ogungbe A.S., Ometan O.O., Ogwala A. (2016). Day to day variability of the critical frequency of F1 layer. International Journal of Advanced in Science Engineering and Technology, Vol. 4(2):212-215.

Tsurutani, B.T., et al. (2006). CIR and CME driven geomagnetic storms. Journal of Geophysical Research.

Yiğit E., Kilcik A., Elias A., G., Dönmez B., Ozguc A., Yurchshyn V. and Rozelot J-P. (2018), Vol. 171, pp. 157-163. https://doi.org/10.1016/j.jastp.2017.11.018

Zerbo, J.-L., Amory-Mazaudier C., Ouattara F. And Richardson. (2012). Solar wind and geomagnetism: toward a standard classification of geomagnetic activity from 1868 to 2009. Annales Geophysicae. 30, 421–426. https://doi.org/10.5194/angeo-30-421-2012